Sains Malaysiana 44(1)(2015): 147–153

Threshold Criteria for Incipient Grain Motion with Turbulent Fluctuations on a Horizontal Bed

(Kriteria Pergerakan Ambang Butiran oleh Fluktuasi Gelora di atas Dasar Mendatar)

W.H.M. WAN MOHTAR*

ABSTRACT

The effect of turbulent fluctuations on the threshold criteria for incipient grain motion over a wide range of sediment size is investigated. In this work, attention is paid to the comparison of the critical Shields parameter θ_c *profile obtained when the near-bed fluid forces induced sediment motion are oscillating-grid turbulence and a single idealised eddy of vortex ring. For experimental work, near-spherical monodisperse sediments were used throughout with relative densities of 1.2 and 2.5 and mean diameters* d *ranging between 80 and 1087 µm. The measured values of* θ_c *on a horizontal bed* $\alpha = 0$ *(hence denoted as* θ_{c0}*), were compared to the* θ_{c0} *profiles obtained by grid turbulence and vortex ring experiments. Although different in magnitude, the* θ_{c0} *profiles were comparable, that is the* θ_{c0} *were seen to increase monotonically for hydraulically smooth bedforms and to be approximately constant for hydraulically rough bedforms. However the limit of hydraulically smooth region was found to vary between the oscillating-grid turbulence experiments, where wider smooth region was found when the turbulent fluctuations used to calculate* θ_{c0} *is not the near-bed velocity.*

Keywords: Hydraulically smooth; incipient grain motion; oscillating-grid turbulence; rough bedforms; vortex ring

ABSTRAK

Kajian ini melihat kesan bentukan gelora ke atas kriteria nilai ambang pergerakan ambang butiran pada satu julat saiz sedimen. Fokus kajian adalah perbandingan profil parameter kritikal Shields θ_c *apabila daya bendalir dekat-dasar bagi sedimen bergerak teraruh oleh turbulens grid-berayun dan pusaran tunggal terunggul cincin vorteks. Uji kaji dilakukan ke atas sedimen seragam berbentuk hampir-sfera dengan ketumpatan relatif sedimen adalah 1.2 dan 2.5 dan diameter purata* d *adalah antara julat 80 dan 1087 µm. Nilai terukur* θ_c *pada dasar mendatar* $\alpha = 0$ *(dengan itu ditandakan sebagai* θ_{c0}*) dibandingkan dengan profil diperoleh bagi kedua-dua eksperimen turbulens grid-berayun dan cincin vorteks. Walaupun nilai terukur berbeza daripada segi magnitud, profil* θ_{c0} *bagi kedua-dua uji kaji adalah sebanding, iaitu* θ_{c0} *bertambah secara ekanada bagi bentuk dasar kelicinan hidraulik dan hampir malar bagi bentuk dasar kekasaran hidraulik. Namun begitu, batasan kawasan kelicinan hidraulik didapati berubah bagi eksperimen grid-berayun dengan daerah kelicinan didapati lebih lebar apabila bentukan gelora diguna pakai untuk mengira* θ_{c0} *bukan halaju hampir-dasar.*

Kata kunci: Bentuk dasar kekasaran; cincin vorteks; kelicinan hidraulik; pergerakan ambang butiran; turbulens grid-berayun

INTRODUCTION

In assessing the transportation of sediment in water streams, one of the most crucial and frequently required parameters is the critical Shields parameter θ_{c0}, the limit of defining the mobility of a particle from its stationary position. The concept of using the θ_{c0} is first formulated by Shields (1936) using dynamic similarity between the bottom shear stresses and the immersed weight of the grains. The parameter θ_{c0} is defined as:

$$\theta_{c0} = \frac{\tau_c}{(\rho_s - \rho) g d}, \quad (1)$$

where $\tau_c = \rho u_{*c}^2$ is the critical bed shear stress; u_{*c} is the critical shear velocity, i.e. a characteristic velocity defined at near-bed region; d is the mean grain diameter; and ρ_s and ρ are the sediment and fluid densities, respectively.

Using τ_c as the critical parameter arises from the fact that in steady uniform flows, the statistics of the near-bed turbulence that induce sediment motion, are scaled with the shear velocity u_{*c}. For decades, most of the characterisation of threshold sediment motion, started from the work of Shields (1936) (i.e. the Shields diagram) and the subsequent improvement of the diagram by Mantz (1977) and Vanoni (1975) used such simplification. However, it has been found that using θ_c obtained from the Shields diagram often yields poor and inconsistent results when applied to real flows or in complex flows (Paintal 1971; Shvidchenko & Pander 2000; Wu et al. 2008). This is due to the fact that in such flows where the simplifications of uniformity and stationarity no longer hold, the intensity of turbulent fluctuations in the near-bed region can vary significantly with bed position and

time. Typical factors causing this non-uniformity and/or intermittency include local variations in bed slope or bed geometry, obstacles within the flow and the presence or development of intermittent coherent vortex structures in the near-bed region (Kaftori et al. 1995; McLean 1994; Nio & Garcia 1996). Under these conditions, the near bed turbulence is no longer correlated with the mean flow characteristics and as such the parametric relation based on steady uniform flows is rendered inaccurate.

A detailed understanding of the interaction of fluctuating forces (i.e. turbulence) with sediment particles is very necessary (Schmeeckle et al. 2007). Recent studies have attempted to address some of these issues by considering the role played by (unsteady) single idealised eddy of vortex ring to a sediment layer (Munro 2012; Munro et al. 2009). Vortex ring is an ensemble of elemental vortex structure, steady and reproducible in the laboratory. One notable advantage of using the vortex ring is that conditions for incipient grain motion can be defined objectively and determined with a high degree of repeatability. Studies of Munro (2012) and Munro et al. (2009) have been conducted on both horizontal and sloping beds, where the critical Shields profiles obtained were qualitatively comparable with the established Shields diagram. However, vortex ring is a laminar flow and only portrays the interaction of a single energetic eddy with a sediment layer, where in real flow, such idealistic form is rarely exist and the eddies are inter-dependent. In this article, the role of turbulent fluctuations is extended by experimentally investigating the interaction of turbulence generated from a vertically oscillating-grid on a sediment layer. Oscillating-grid turbulence consists of continual multiple interacting energetic eddies from the production region to the near-bed region. The flow produced has an approximation of zero mean fluid velocities, thereby allowing the effect of turbulent fluctuations to be considered in isolation.

The flow generated is a quasi-isotropic, laterally homogeneous turbulence and at distances further away from the grid, the decay of (time-averaged) root mean square (r.m.s) tangential velocity components (u,v) with depth below the grid's mid position Z, can be expressed as:

$$u = v = CfS^{3/2} M^{1/2} Z^{-1}, \quad (2)$$

where f is the oscillation frequency; S is the stroke; M is the mesh size and the dimensionless constant (Cheng & Law 2007; Hopfinger & Toly 1976). This equation is (only) applicable at $Z \gtrsim 2.5M$, a region considered to reach the state of quasi-isotropic homogeneous turbulence (Hopfinger & Toly 1976). Several studies have employed oscillating-grid turbulence to investigate the threshold criteria for sediment movement, in particular the work of Bellinsky et al. (2005) and Wan Mohtar and Munro (2013).

This article is set to qualitatively compare the role played by turbulent fluctuations on the overall trend of θ_{c0} measured by turbulent fluctuations of grid turbulence and vortex ring. One should bear in mind that the nature of both flows are different in that vortex ring is a steady laminar single eddy whereas the oscillating-grid turbulence produces multiple random eddies interacting with each other throughout the whole distance from the grid to the sediment bed. Although the method of generating turbulence and the initial state of the turbulence structure is different, both methods are representative of turbulent fluctuations without significant influence from the mean flow.

Experimental Details

The physical properties of the sediment types used in the experiments will be first described and followed by how the oscillating-grid turbulence was used to measure the threshold criteria for each sediment type. For the experimental setup, methods and velocity measurement for the threshold sediment motion by vortex ring, detailed explanation is referred to the work of Munro (2012).

Two different monodisperse sediment types were used, namely glass ballotini and diakon, with relative density $s = \frac{\rho_s}{\rho} = 2.5$ and 1.18, respectively, where ρ_s and ρ are sediment and fluid densities, respectively. The basic properties of the particles are listed in Table 1, where d, s, σ_d and φ denote the mean particle diameter, relative density, the terminal settling velocity of a single particle, sediment gradation parameter and the angle of

TABLE 1. The physical characteristics of sediment used

Label	Material	d (μm)	s	Re_p	σ_d	φ (°)
A	Glass	1101.5	2.5	137.0	1.07	27.5
B	Glass	716.1		72.4	1.11	28.2
C	Glass	562.6		51.2	1.14	28.8
D	Glass	373.9		27.7	1.16	28.1
E	Glass	220.3		12.5	1.20	30.4
F	Glass	153.3		7.3	1.15	29.1
G	Glass	80.0		2.7	1.29	29.0
H	Diakon	751.1	1.18	79.0	1.13	30.8
I	Diakon	273.8		17.4	1.27	33.1
J	Diakon	157.8		7.6	1.10	32.2
K	Diakon	118.7		5.0	1.24	28.9

repose (in water), respectively. Each sediment type is presented as a dimensionless particle Reynolds number $Re_p = \sqrt{(\rho_s - \rho) g d^3 / \nu}$, where ν is the water kinematic viscosity. Each sediment used was nearly spherical and homogeneously distributed with a narrow size distribution about mean diameter, with values of $\sigma_d < 1.4$ for all sediment types. Note that the same sediment types were also used for the vortex ring experiments.

The experiments were performed in an acrylic tank, with cross-sectional dimensions of 35.4 × 35.4 cm^2 and a height of 50 cm. The tank is fixed within a rigid inner steel frame (as shown in Figure 1(a)) and filled with water to a depth of 40 cm. The oscillating-grid mechanism, consisting of a linear bearing was positioned vertically through the central axis of the tank and connected to a rotating spindle. A motor was used to rotate the spindle and thus continuously oscillate the grid. The plan view of the square (d_g = 1 cm) uniform grid is shown in Figure 1(b) made from 7×7 array of aluminium bars and length of 35 cm. The uniform mesh size M is 5 cm and gives the grid a solidity of 36%. The end condition of the grid was designed to ensure that the wall acted as a plane of reflection-symmetry, which has been shown to lessen the Reynolds-stress gradients within the fluid, thereby inhibiting the presence of undesirable secondary circulations (Fernando & DeSilva (1993). The opening between the wall and the grid is approximately 2 mm, which is too small to cause any significant secondary circulation (Voropayev & Fernando 1996). In a preliminary series of experiments, the turbulence intensity u/U and w/W is found typically between 2 and 4, giving the fluctuations are always dominant compared with the mean components and so the secondary flow has insignificant impact on the incipient sediment motion. Note that the symbols U and W are the horizontal and normal mean velocity components in the quasi-isotropic homogeneous region, respectively.

To ensure that the threshold conditions for each sediment type are consistent, each experiment was performed with the stroke fixed at S = 8 cm and distance from grid mid-position fixed at $Z = 3.2M$ (16 cm). For each sediment type, a sediment layer was formed in a 33 cm square tray, 1 cm deep, fixed in position at the base of the tank. The sediment layer was formed by carefully drawing a flat scraper across the top rim of the tray, which produced a flat, close-packed bed of consistent mean depth 1 cm. Once the sediment bed was set, the frequency of oscillation f was gradually increased from 0.5 Hz with ≈ 0.25 Hz increments until the threshold particle movement was observed through visualisation. For each frequency increment, the turbulent flow was allowed to develop for approximately 1 min before being further increased, thereby allowing the turbulence to reach a new steady state. The 'critical' frequency f_c was recorded when intermittent sediment movements were observed at each quadrant of the bed for duration of 10 s. In order to minimise the error, each of the experiments was repeated and the threshold conditions were recorded at least five times for each sediment type and bed slope. During the procedure, the sediment layer was re-scraped and flattened prior to repeating each test.

Once the critical frequency had been identified for a given sediment type, time-resolved measurements of the grid-turbulence (interacting with the bed) were then obtained using a two-dimensional planar Particle Image Velocimetry (PIV). The fluid velocity measurements were sampled at 200 Hz using a Dantec NanoSense MkIII digital camera (with 1280×1024 pixel resolution) for a period of T = 90s. The velocity fields were calculated directly from the captured images using standard PIV software. The interrogation area was set at 20×20 pixels (equivalent to 0.019×0.019 cm) with a 50% overlap between the analysis spots. In each experiment, the PIV images captured the region between the bottoms of the grid to the sediment bed, giving a physical area of 3.2 M × 4M cm^2.

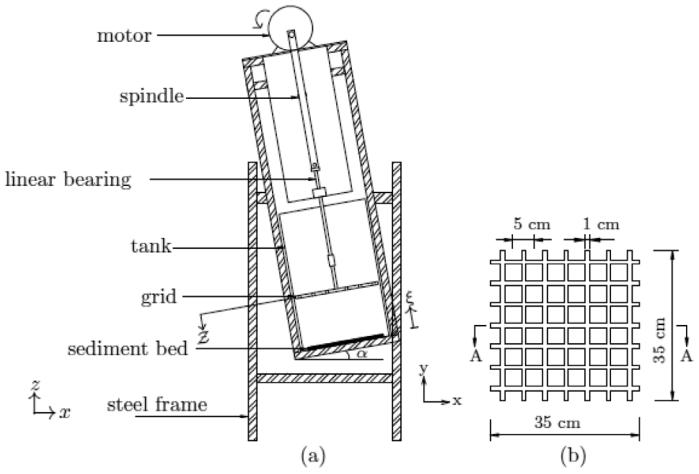

FIGURE 1. Sketches showing (a) the experimental setup and (b) a (magnified) plan-view of the uniform grid. A sediment bed is placed at the bottom of the tank. The symbol ξ denotes the distance from sediment bed, where ξ= 0 is the bed surface

Results and Discussion

Characterising the critical velocity

The values of θ_{c0} can be predicted from the traditional Shields diagram or adopting the abundant empirical θ_{c0} equations (Camenen & Larson 2005). Such estimates are typically based on thresholds for incipient sediment motion in a steady turbulent channel flow, in which case the mean velocity profile is well understood and the τ_c for (1) can be estimated using standard formulae e.g. $\tau_c = \rho gHS$, where H is the hydraulic depth and S is the channel slope. For the experiments described here and threshold criteria by vortex ring, the measurement of τ_c was not possible and thus an alternative estimate for τ_c was required, based on the available fluid velocity data.

A typical turbulent profile (of rms horizontal u and vertical w velocity components) at near-bed region i.e. from $\xi/l_0 = 0 - 2$, where ξ is the distance above the bed surface and $\xi = 0$ is the bed, is shown in Figure 2. The symbol $\langle\rangle$ denotes spatially averaged values across horizontal direction. The values are made dimensionless with the values of u_0, w_0 and l_0, that is the values measured at depth $Z = 2.5\,M$, a distance regarded as the quasi-isotropic homogeneous region.

It is evident from Figure 2 that the presence of sediment bed significantly changes the (initial quasi-isotropic homogeneous) turbulence structure, leading to anisotropy in the near-bed region $0 < \xi/l_0 \lesssim 1$. The r.m.s vertical velocity w component monotonically decreases as $\xi \to 0$, due to the kinematic boundary condition induced by the presence of the sediment bed. In contrast, the r.m.s horizontal velocity u component experiences amplification between $0.2 \leq \xi/l_0 \leq 1$, attaining a peak value at $\xi/l_0 \approx 0.3$ due to the inter-component energy transfer (Bodart et al. 2010). From there, u decreases to zero at the sediment bed to satisfy the no slip condition. The turbulent profile obtained is similar to that obtained in previous studies of zero mean turbulence at near solid boundary (Aronson et al. 1997; Bodart et al. 2010; Perot & Moin 1995).

Under critical conditions for incipient motion, near-surface sediment grains are displaced by the action of the hydrodynamic drag and lift forces induced by the tangential fluid velocity components at near-bed. It is standard for the sediment threshold criteria to be prescribed in terms of a characteristic scale for the critical bed shear stress τ_c. In previous studies, Bellinsky et al. (2005) and Medina (2002) employed oscillating-grid turbulence to measure the sediment incipient motion and obtained the values of θ_{c0} either from (2) or using the measured r.m.s horizontal velocity taken at the homogeneous region. Obviously, they did not account for the changes of turbulence structure due to the presence of sediment bed as evidently shown in Figure 2. The use of both approaches does not give an accurate representation of the actual forces acting on the particles, as the velocity scales calculated using (2) ignores the occurrence of inhomogeneity and the measurement taken at the homogeneous region is underestimated. Here the analysis approach is made more rigorous by considering how the presence of bedform affected the statistical properties of the turbulence in the near-bed region.

Thus, taking into account the changes of turbulence structure at the near-bed region, a different approach to determine the critical velocity was undertaken in this study. Let $\langle u\rangle_b$ denote the horizontal fluid velocity component measured at the amplification point (typically at $\xi/l_0 = 0.3$), during the interaction period. The $\langle u\rangle_b$ measured at this distance, which is close to the bed surface, is a reliable velocity measurement and could be consistently obtained using the PIV set up described. Under the critical impact conditions, sediment grains are brought into motion only by the peak value of the bed shear stress, which is expected to scale with $\tau_c \sim \rho\langle u\rangle_b^2$. Hence, in the present context, the critical Shields parameter was defined as,

$$\theta_c = \frac{\langle u\rangle_b^2}{(s-1)dg}. \tag{3}$$

To minimise error associated with $\langle u\rangle_b$, each $\langle u\rangle_b$ values were taken by averaging from (at least) five measurements.

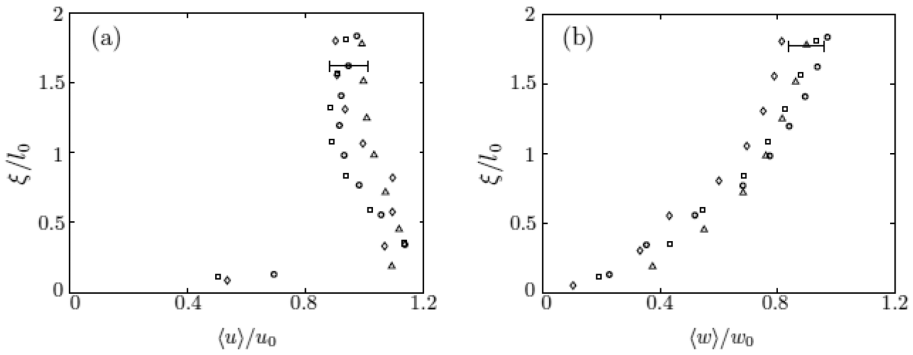

FIGURE 2. Plots showing measured values of spatially averaged r.m.s (a) horizontal and (b) vertical velocity components against dimensionless height $\xi = l_0$ above the sediment bed surface. Data correspond to $S = 8$ cm with varying frequency $0.9 \leq f < 3$ Hz. Four sets of data shown correspond to $f = 2.32$ (∘), $f = 2.15$ (□), $f = 1.68$ (Δ) and $f = 1{:}44$ (◇), respectively. To avoid saturation, a single error bar has been included that is representative of the variability observed in all of the data shown

Utilising the peak value of $\langle u \rangle_b$ (at $\xi \approx 0.3$–0.4) is a representative of the most energetic turbulent eddies in the near-bed region.

INCIPIENT SEDIMENT MOTION

Figure 3 shows the values of θ_{c0} plotted against particle Reynolds number Re_p, for each of the eleven sediment types. Separate data symbols have been used to differentiate between diakon ($s = 1.18$) and ballotini ($s = 2.5$) sediments. The error bars of θ_{c0} are based on the typical variability of $\langle u \rangle_b$, where the value of $\langle u \rangle_b$ is averaged over five measurements.

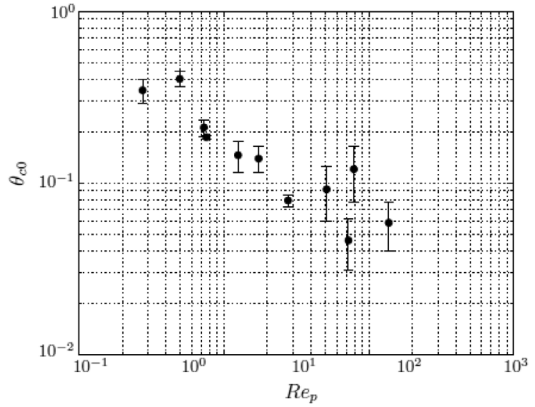

FIGURE 3. Measured values of critical Shields parameter θ_c against Re_p. Vertical error bars show the variability in the measured values of $\langle u \rangle_b$

Although the θ_{c0} reported in Figure 3 were not obtained using u_{*c} as in the critical shear velocity in steady turbulent channel flows, a number of qualitative consistencies can be identified. In particular, White (1970) classified bedforms under threshold conditions, where the critical diameter is set at 200 μm, below is hydraulically smooth and above is hydraulically rough bedforms. For the experiments considered here, a hydraulically rough bedform corresponds to when the roughness length-scale (k_s), usually expressed as the diameter size d for uniform-size sediment, is comparable to (or larger than) the boundary-layer depth. For a hydraulically smooth bedform, k_s is significantly smaller than the boundary-layer depth, allowing a laminar viscous sublayer to be established in the fluid immediately above the bed surface, within which viscous stresses act to significantly reduce the drag and lift forces acting on the exposed surface sediment. Within this regime, the critical Shields parameter is found to increase significantly with decreasing sediment size (i.e. Re_p), due to the damping effect of the viscous sublayer (White 1970). Conversely, when d increases and the flow near-bed becomes hydraulically rough, this viscous damping effect ceases to be evident and the critical Shields parameter is found to vary very little with Re_p (and is constant for $Re_p > 70$ (i.e. $d \geq 3$ mm for natural sediments)) (Lamb et al. 2008). Despite general scatter, a similar pattern can be identified in the data reported in Figure 3. That is, for $Re_p \leq 20$ the measured values of θ_{c0} increase monotonically with decreasing Re_p, whereas for $Re_p > 20$, $\theta_{c0} \approx 0.05$ (and near-constant), which suggests that, here, the viscous damping effect becomes significant for $Re_p \leq 20$. That is, the limit of hydraulically smooth is set at $Re_p \approx 20$, equivalent to $d \approx 290$ μm, comparable with the critical diameter set by White (1970). Also note that in Figure 3, within the range of available Re_p, $\theta_{c0} \approx 0.4$ for the finest sediment, whereas $\theta_{c0} \approx 0.05$ for the larger grain sizes. This factor of eight differences is the same as that reported in White (1970) for comparable grain sizes.

Note that, for fine-grained sediments, cohesive forces can become dominant in comparison with the grain weight. However, this situation occurs only for very fine particles with $d \gtrsim 30$ μm considerably smaller than the grain sizes used here (Phillips 1980). Hence, here, the effects of cohesion have been ignored throughout.

For comparison, data from experiments of oscillating-grid and vortex ring experiments (herein after referred to as OG and VR), respectively, against dimensionless Re_p is plotted in Figure 4. It is informative to first focus attention on the measurements of θ_{c0} with those obtained from previous incipient motion using oscillating-grid, here compared with data from Bellinsky et al. (2005). Separate data symbols have been used to differentiate between θ_{c0} obtained in this study and Bellinsky's (i.e. full ∘ and ◇), respectively. They studied a (wider) range of particle sizes $1 \leq Re_p \leq 370$, which includes both hydraulically smooth and rough regimes. Although similar θ_{c0} profiles were obtained, it has been noted that for $Re_p > 40$, the data of Bellinsky reached a (relatively) constant $\theta_{c0} \approx 0.03$ value, much lower than the data reported here. Quantitatively, within Re_p ranges, all Bellinksy's data have lower values than those measured in this study. This is due to the difference in the θ_{c0} calculation where they defined the critical bed shear stress $\tau_c \sim \rho u_c$, and u_c is calculated using (2). The value u_c taken at the homogeneous region ignored the inhomogeneity within the boundary layer and the amplification of u in the near-bed region, thus resulting in an underestimate values of θ_{c0}. At $Re_p \lesssim 40$, the sediment size falls under the hydraulically smooth, where the viscous forces become significant. The θ_{c0} values monotonically increased as the Re_p decreased.

The focus now is paid to the comparison of measured θ_{c0} with the values obtained from the vortex ring experiments. Note that in Figure 4, θ_{c0} obtained in VR experiments are presented with symbol □. The measured θ_{c0} are two orders of magnitude larger than the profile obtained from the OG experiments, which is expected due to the differences in the velocity scale used in obtaining the θ_{c0}. In the VR experiments, the absolute peak fluid velocity at near-bed was used and of course will give essentially higher θ_{c0} values than when calculated using r.m.s fluid velocity (for OG experiments). Therefore, a direct quantitative comparison is precluded. However, a number of qualitative consistencies can be identified. For the hydraulically smooth region where $Re_p \lesssim 20$,

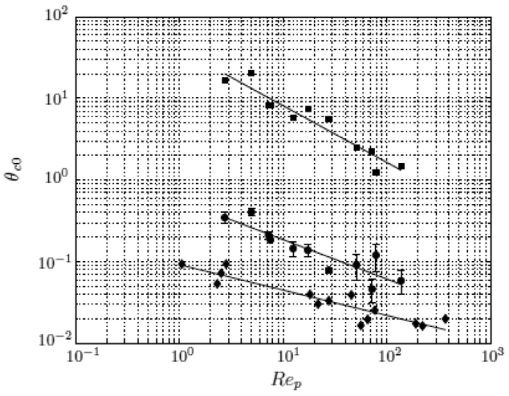

FIGURE 4. The measured critical Shields parameter θ_{c0} plotted together with data extracted from Bellinsky (2005) and Munro (2012). The different data point styles (all legends are put black) represent this study (◦), Bellinsky (◇) and Munro (□)

the measured values of θ_{c0} increase monotonically with decreasing Re_p, whereas for $Re_p > 20$, θ_c reaches a near-constant value at $\theta_{c0} \approx 2$. The data also show that the factor of five differences is achieved between the measured θ_{c0} in rough and smooth flow regimes, which is the same as reported in White (1970) for comparable grain sizes.

It is noticed that the boundary of hydraulically smooth to rough between the OG experiments (that is this study and Bellinksy's) are varies. Data of Bellinksy shows that condition of grain independence, reached to a larger size of sediment at $Re_p > 40$. The θ_{c0} reached to a constant value for sediment sizes $d \lesssim 460$ μm, much larger compared with our data of $d \lesssim 290$ μm. Using (2) to define the critical velocity not only underestimating the θ_{c0} value, but also resulted in a wider hydraulically smooth region. Wider region implicates the water-induced erosive process (for sediment within the region) might be underestimated. That is, for example, when the sediment is erroneously falls as hydraulically smooth, the sediment is expected to be more difficult to be entrained due to the significant effect from the viscous force, where as in reality, the viscous force plays a minimal role and the sediment is more easily entrained into the flow.

The analysis implies that it is difficult to identify the limit of hydraulically smooth and rough as the characterisation of incipient sediment motion depends on both the subjectivity of the definition of incipient motion and the temporal fluctuating forces acting on the particle (Buffington & Montgomery 1997). The ambiguity definition of both incipient sediment motion and critical velocity contributes to the inconsistent of the Re_p limit between smooth and rough region although similar flow generation (where in this case is grid turbulence) was used.

CONCLUSION

The experiments reported here examined the threshold criteria of sediment grains when a sediment layer is made to interact with zero-mean oscillating-grid turbulence. The attention is focused on how the critical Shields parameter θ_c profiles over the range of particle Reynolds number $0 < Re_p \leq 370$ exhibit when the dominant fluid forces induced incipient sediment motion are attributed from turbulent fluctuations. The measured θ_{c0} were made to compare with two type of turbulent fluctuations. One is with oscillating-grid turbulence where the comparisons were with the data extracted from Bellinsky et al. (2005). Second is with θ_{c0} obtained from the experiments of Munro (2012), interacting an idealised vortex ring onto a sediment layer. Vortex ring is an idealised coherent vortex structure and is a representation of turbulent eddies without contribution from mean flow, similar concept as using the oscillating-grid turbulence. Since θ_{c0} was not available for both OG and VR experiments, θ_c was defined using a velocity scale characteristic of the peak variation in the near-bed region during the interaction period.

The measured values of θ_{c0} at horizontal bed identified similar qualitative trends when compared with both data obtained in grid turbulence and vortex ring experiments. Although notably different in magnitude, the measured θ_{c0} profiles show that below the hydraulically smooth region, the bed roughness effect becomes evident and so the viscous stresses (within the viscous sublayer) effectively reduces hydrodynamic forces acting on the bed surface. Consequently, the θ_{c0} were observed to increase monotonically as Re_p decreases. Above the smooth region, sediment grains are much larger than the viscous sublayer and the effect of viscous damping is minimal. However, the limit where the smooth region starts vary where wider region was identified for Bellinsky's data. This was due to the lower turbulence intensity used to define the θ_{c0} and the u_c used is not an actual representation of the near-bed velocity.

The main difference employed in this study, compared with the usually employed turbulent flow in a steady channel, is that the turbulence intensity level (in terms of the horizontal component) to characterise the incipient sediment motion is $u/\bar{U} > \mathcal{O}(1)$, where $\bar{U}$ is the mean horizontal velocity, whereas in the developed traditional Shields diagram, the turbulence intensity level is $u/\bar{U} \leq \mathcal{O}(1)$. Although the turbulent fluctuations were used to characterise the θ_c, comparable profiles with the traditional Shields curve is due to the statistically stationary and laminar flows of grid turbulence and vortex ring, respectively.

REFERENCES

Aronson, D., Johansson, A. & Lofdahl, L. 1997. Shear-free turbulence near a wall. *J. Fluid Mech*. 338: 363-385.

Bellinsky, M., Rubin, H., Agnon, Y., Kit, E. & Atkinson, J. 2005. Characteristics of resuspension, settling and diffusion of particulate matter in a water column. *Env. Fluid. Mech*. 5: 415-441.

Bodart, J., Cazalbou, J. & Joly, L. 2010. Direct numerical simulation of unsheared turbulence diffusing toward a free-slip or no-slip surface. *J. Turbulence*. 11: 1-17.

Buffington, J.M. & Montgomery, D. 1997. A systematic analysis of eight decades of incipient motion studies, with special reference to gravel-bedded rivers. *Water Res*. 33: 1993-2029.

Camenen, B. & Larson, M. 2005. A general formula for non-cohesive bed load sediment transport. *Est. Coast. and Shelf Sci*. 63: 249-260.

Cheng, N.S. & Law, A.W.K. 2007. Measurements of turbulence generated by oscillating grid. *J. Hyd. Eng*. 127: 201-207.

Fernando, H.J.S. & DeSilva, I.P.D.D. 1993. Note on secondary flows in oscillating-grid, mixing-box experiments. *Phys. Fluids* 5: 1849-1851.

Hopfinger, E.J. & Toly, J.A. 1976. Spatially decaying turbulence and its relation to mixing across density interfaces. *J. Fluid Mech*. 78: 155-175.

Kaftori, D., Hetsroni, G. & Banerjee, S. 1995. Particle behavior in the turbulent boundary layer. i. motion, deposition and entrainment. *Phys. Fluids* 7: 1095-1105.

Lamb, M.P., Dietrich, W.E. & Venditti, J.G. 2008. Is the critical shields stress for incipient sediment motion dependent on channel-bed slope? *J. Geophys. Res*. 113: 1-20.

Mantz, P. 1977. Incipient transport of fine grains and flakes by fluids-extended shields diagram. *J. Hydr. Div*. 103: 601-615.

McLean, S. 1994. Turbulence structure over two-dimensional bed forms: Implications for sediment transport. *J. Geoph*. 99: 729-747.

Medina, P. 2002. Start of sediment motion and resuspension in turbulent ows: Applications of zero-mean ow grid stirred turbulence on sediment studies. PhD Thesis. Universidad Polit´ecnica de Catalu˜na. (Unpublished).

Munro, R.J. 2012. The interaction of a vortex ring with a sloped sediment layer: Critical criteria for incipient grain motion. *Phys. Fluids* 24: 026604.

Munro, R.J., Bethke, N. & Dalziel, S.B. 2009. Sediment resuspension and erosion by vortex rings. *Phys. Fluids* 21: 1-16.

Ni˜no, Y. & Garcia, M.H. 1996. Experiments on particle-turbulence interactions in the near-wall region of an open channel flow: Implications for sediment transport. *J. Fluid Mech*. 326: 285-319.

Paintal, A. 1971. Concept of critical shear stress in loose boundary open channels. *J. Hydr. Res*. 9: 91-113.

Perot, B. & Moin, P. 1995. Shear-free turbulent boundary layers. part 1. Physical insights into near-wall turbulence. *J. Fluid Mech*. 295: 199-227.

Phillips, M. 1980. A force balance model for particle entrainment into a fluid stream. *J. Phys. D: App. Phys*. 13: 221-233.

Schmeeckle, M., Nelson, J. & Shreve, R. 2007. Forces on stationary particles in near-bed turbulent flows. *J. Geophys. Res*. 112: F02003.

Shields, A. 1936. Application of similarity principles and turbulence research in bed-load movement. In *Hydrodyna-Mics Laboratory Publ. no. 167*, edited by Ott, W.P. & van Uchelen, J.C. US Dept of Agr., Soil Conservation Service Cooperative Library, California Institute of Technology, Pasadena, Calif.

Shvidchenko, A.B. & Pander, G. 2000. Flume study of the effect of relative depth on the incipient motion of coarse uniform sediments. *Water Res*. 36: 619-628.

Vanoni, V. 1975. *Sedimentation Engineering*. American Society of Civil Engineers Publications.

Voropayev, S. & Fernando, H.J.S. 1996. Propagation of grid turbulence in homegeneous fluids. *Phys. Fluids* 8: 2435-2440.

Wan Mohtar, W.H.M. & Munro, R.J. 2013. Threshold criteria for incipient sediment motion on an inclined bedform in the presence of oscillating-grid turbulence. *Phys. Fluids* 25: 015103.

White, S.J. 1970. Plane bed tresholds for fine grained sediments. *Nature* 228: 152-153.

Wu, B., Maren, D. & Li, L. 2008. Predictability of sediment transport in the yellow river using selected transport formula. *Int. J. Sed. Res*. 23: 283-298.

Department of Civil & Structural Engineering
Faculty of Engineering and Built Environment
Universiti Kebangsaan Malaysia
43600 Bangi, Selangor Darul Ehsan
Malaysia

*Corresponding author; email: hanna@ukm.edu.my

Received: 23 September 2013
Accepted: 31 May 2014